eNeuro

Research Article: New Research | Cognition and Behavior

Noninvasive brain stimulation enhances memory acquisition and is associated with synaptoneurosome modification in the rat hippocampus

https://doi.org/10.1523/ENEURO.0311-19.2019

Cite as: eNeuro 2019; 10.1523/ENEURO.0311-19.2019

Received: 6 August 2019
Revised: 15 October 2019
Accepted: 31 October 2019

Noninvasive brain stimulation enhances memory acquisition and is associated with synaptoneurosome modification in the rat hippocampus

Abbreviated Title: tDCS enhances memory acquisition and proteome

Seung Ho Jung[1, 2, 3*], Candice Hatcher-Solis[1], Raquel Moore[1, 4], Naomi Bechmann[1, 4], Sean Harshman[5, 6], Jennifer Martin[6] & Ryan Jankord[1]

Affiliations:
[1]Applied Neuroscience Branch, 711th Human Performance Wing, Air Force Research Laboratory, Wright-Patterson AFB, OH 45433, USA
[2]Research Associateship Program, National Research Council, National Academies of Science, Washington, DC 200001, USA
[3]ORISE, 100 Orau Way, Oak Ridge, Tennessee 37830
[4]Infoscitex, 4067 Colonel Glen Hwy Suite 210, Dayton, Ohio 45431, USA
[5]UES, Inc., 4401 Dayton Xenia Rd, Dayton, OH 45432, USA
[6]Human Signatures Branch, 711th Human Performance Wing, Air Force Research Laboratory, Wright-Patterson AFB, OH 45433, USA

***Corresponding Author**: Seung Ho Jung, Ph.D.
Applied Neuroscience
Warfighter Interface Division
711th Human Performance Wing
Air Force Research Laboratory
Wright-Patterson AFB, OH 45433
Office: 937-938-3683
Fax: 937-656-6894
Email: seung.jung.ctr@us.af.mil; seung.jung@gmail.com

Number of Figures: 5
Number of Tables: 3
Extended Data: 3 Figures & 8 Excel files
Number of Words for Abstract: 238
Number of Words for Significance Statement: 93
Number of Words for Introduction: 586
Number of Words for Discussion: 1586

Acknowledgments: The authors would like to thank Sylvia Cunningham and the Wright-Patterson Air Force Base Research Support Command for their contribution to this work.

Conflicts of interest: All authors confirm that there are no known conflicts of interest related to this manuscript.

Funding sources: This work was supported by the Air Force Office of Scientific Research (AFOSR grant numbers 13RH14COR and 16RHCOR362) and has been approved for public release (Distribution A: Approved for public release. 88ABW Cleared 05/July/2019; 88ABW-2019-3239).

ABSTRACT

Transcranial direct current stimulation (tDCS) is a non-invasive brain stimulation approach previously shown to enhance memory acquisition, but more studies are needed to elucidate the underlying mechanisms. Here, we examined the effects of anodal tDCS (0.25 mA for 30 minutes) on the memory performance of male Sprague Dawley rats in the passive avoidance test (PAT) and the associated modifications to the hippocampal proteomes. Results indicate anodal tDCS applied before the acquisition period significantly enhanced memory performance in the PAT. Following passive avoidance testing, synaptoneurosomes were biochemically purified from the hippocampi of tDCS- or sham-treated rats and individual protein abundances were determined by bottom-up liquid chromatography mass spectrometry analysis. Proteomic analysis identified 184 differentially expressed hippocampal proteins when comparing the sham to the tDCS before memory acquisition treatment group. Ingenuity pathway analysis (IPA) showed anodal tDCS before memory acquisition significantly enhanced pathways associated with memory, cognition, learning, transmission, neuritogenesis, and long-term potentiation. IPA identified significant upstream regulators including *bdnf*, *shank3*, and *gsk3b*. Protein-protein interaction and protein sequence similarity networks show that glutamate receptor pathways, ion channel activity, memory, learning, cognition and long-term memory were significantly associated with anodal tDCS. Centrality measures from both networks identified key proteins including *dlg*, *shank*, *grin*, and *gria* that were significantly modified by tDCS applied before the acquisition period. Together, our results provide descriptive molecular evidence that anodal tDCS enhances memory performance in the passive avoidance test by modifying hippocampal synaptic plasticity related proteins.

SIGNIFICANCE STATEMENT

We investigated whether anodal tDCS affects memory performance and the underlying protein modifications in hippocampal synaptoneurosomes. We found that anodal tDCS administered before

memory acquisition significantly enhanced memory performance by enhancing the expression of hippocampal proteins associated with glutamate signaling and ion channel activity. Our results identify molecular targets for tDCS-induced memory enhancement and the associated signaling pathways. Our behavioral and proteomics study further elucidates the mechanism for tDCS effects on acquisition memory and may lead to the development of therapeutics to enhance memory and learning process for neurological diseases and psychological disorders.

INTRODUCTION

Transcranial direct-current stimulation (tDCS) is widely utilized clinically due to its non-invasive application and few reported side effects (Stagg and Nitsche, 2011; Holmes et al., 2016). Clinical studies have revealed the beneficial effects of tDCS as a therapeutic tool for neurological diseases and psychological disorders including Alzheimer's disease, schizophrenia, depression, and anxiety (Marshall et al., 2004; Boggio et al., 2006; Goder et al., 2013; Ladenbauer et al., 2017; Hill et al., 2018; Medvedeva et al., 2019). Although the biological and molecular mechanisms remain unclear, tDCS has been shown to enhance memory. tDCS improves working memory (Hoy et al., 2013; Martin et al., 2014; Bogdanov and Schwabe, 2016), long-term memory (Javadi and Cheng, 2013), semantic memory (Cattaneo et al., 2011; Holland et al., 2011), and memory acquisition (Jacobson et al., 2012; Javadi and Walsh, 2012). Moreover, a study using elderly subjects showed that anodal tDCS significantly enhanced memory recall one week after learning compared to sham stimulation, suggesting long lasting effects of tDCS (Floel et al., 2012). Although studies have shown that tDCS enhances memory, especially memory acquisition, there is limited biological data available for the underlying effects of tDCS on the hippocampal proteome, which may explain how tDCS induces memory enhancement.

Several studies in humans and animals have examined the effects of tDCS on neuronal activity and synaptic plasticity to understand the regulatory mechanisms. Electrophysiological studies have

revealed that tDCS increases cortical excitability in humans (Alonzo et al., 2012; Romero Lauro et al., 2014; Bailey et al., 2016). Animal studies have shown that tDCS enhances synaptic plasticity in the hippocampus of rodents (Rohan et al., 2015; Podda et al., 2016). However, the molecular mechanisms of tDCS to enhance memory and learning are less known. tDCS has been shown to affect the expression of immediate early genes *c-fos* and *zif268* in the hippocampus (Ranieri et al., 2012). Studies have further determined that tDCS affects the mRNA level of hippocampal brain-derived neurotrophic factor (BDNF), a growth factor important for long-term memory (Podda et al., 2016; Kim et al., 2017). Additional studies indicate tDCS may regulate neurotransmitter signaling of glutamatergic, GABAergic and cholinergic pathways (Rossini et al., 2015; Giordano et al., 2017) that favor enhancement of memory and cognition. tDCS has also been shown to modify the expression of genes related to serotonergic, adrenergic, dopaminergic, GABAergic and glutamatergic signaling in the rat cortical transcriptome (Holmes et al., 2016). A more recent study showed that tDCS modifies AMPA receptor phosphorylation and translocation in the rat hippocampus (Stafford et al., 2018), suggesting a possible effect of tDCS on protein modifications in rat hippocampal synaptoneurosomes. Another study reports that anodal tDCS enhances performance in the hippocampal-dependent passive avoidance memory task and that the tDCS-induced enhancement was abrogated with pretreatment of ANA-12, an inhibitor of the BDNF receptor tropomyosin receptor kinase B (Yu et al., 2019). More studies are needed to associate tDCS-induced effects on hippocampal protein regulation with behavioral performance to determine mechanism.

In this study, we examined if anodal tDCS affected memory acquisition and/or recall along with the molecular modifications of stimulation on synaptic proteomics in the rat hippocampus. We show that anodal tDCS (250 μA for 30 minutes) applied before the memory acquisition period of a learning and memory test enhances cognitive performance. We report that the enhancement of memory acquisition by anodal tDCS is significantly related to molecular alterations in the hippocampal proteome. The tDCS-induced modifications in hippocampal synaptoneurosomes are significantly associated with receptor

signaling and voltage-gated ion channel activity in pathways associated with learning, memory, and cognitive enhancement.

MATERIALS AND METHODS

Animals

Adult Sprague Dawley rats (male, 7-8 weeks old weighing approximately 400-500 grams, n = 14/group) were purchased from Charles River Laboratories. Rats were housed in the animal facility of the Wright-Patterson Air Force Base (WPAFB) with *ad libitum* access to food and water and maintained on a 12:12 hour light-dark cycle. Rats received a 10 day acclimation period before surgical electrode placement. All rats were maintained according to National Institutes of Health and WPAFB Institutional Animal Care and Use Committee guidelines. The study protocol was reviewed and approved in compliance with the Animal Welfare Act and with all applicable federal regulations governing the protection of animals in research.

Surgical implantation of cranial electrode

Animals were anesthetized with isoflurane (Med-Vet International, Mettawa, IL) using 5% induction, followed by 2–3% isoflurane to maintain anesthetic depth. A 5 mm diameter, circular, head electrode casing (Tangible Solutions, Fairborn, OH) was attached to the skull from 0 mm to -5 mm bregma. Luting dental cement (GC Fuji I, GC America Inc., Alsip, IL) was applied to the base of the head electrode casing and to the skull, followed by an acrylic dental cement (Sigma-Aldrich, St. Louis, MO) to secure the electrode casing. Animals were given a minimum of 7 days as a recovery period before tDCS treatment. Rats were randomly selected for sham, anodal tDCS before acquisition, or anodal tDCS before memory recall.

144 ***tDCS application***

145 On the same day, prior to stimulation, animals were acclimated to the testing room for 10
146 minutes. A conducting medium (SignaGel, Parker Laboratories, Fairfield, NJ) was placed into the head
147 casing prior to connecting the head electrode. The reference electrode (12 mm diameter, Tangible
148 Solutions, Fairborn, OH) was placed on the rat's shaved chest with SignaGel as the conducting medium.
149 Once the electrodes were in place, the animal was wrapped with a flexible cohesive bandage (PetFlex,
150 Med-Vet, Mettawa, IL.) and placed into their home cage. Anodal tDCS was then applied at 0.25 mA
151 using a constant-current stimulator (Magstim DCstimulator; Neuroconn, Ilmenau, Germany) for 30 min.
152 The sham group was prepared the same way as the stimulation groups but did not receive any current
153 (Figure 1).
154
155 ***Behavioral tests***
156 To assess memory acquisition and recall following tDCS, a modified passive avoidance test
157 (PAT) was run as a learning and memory test (Figure 1). Prior to behavioral testing, animals were
158 allowed to acclimate to the testing room for at least 10 minutes. On Day 1 (Habituation), animals had
159 their midsection wrapped in Petflex tape and were returned to their home cage for 20 minutes. They were
160 then unwrapped and placed into an open arena and allowed to explore freely for 5 minutes. Immediately
161 following exploration, animals were then taken to the PAT chamber and allowed to freely explore both
162 rooms for 5 minutes.
163 Approximately 24 hours later (Training, Day 2), animals were wrapped for stimulation and
164 placed in their homecage. Only the group designated to receive stimulation before memory acquisition
165 received anodal tDCS, and the other two groups received sham stimulation. After the 30 minute
166 stimulation period, animals were unwrapped and placed in the open arena on the opposite wall facing
167 away from the two identical objects present. They were allowed to freely explore the arena for a total
168 duration of 3 minutes. They were then taken to the PAT chamber (Gemini, San Diego Instruments, Inc.,
169 San Diego, CA) and placed into a lit room facing away from the gate that led to a dark chamber. After a

30 second acclimation period, the gate rose, and the animal was given the opportunity to cross over to the dark room. Once the animal crossed over, the gate was immediately closed, and after 3 seconds the rat received 0.75 mA shock to the feet for 1 second. After the shock was administered, the rat remained in the dark room for 30 seconds before being removed and returned to its homecage.

Approximately 24 hours later (Testing, Day 3), the animals were wrapped for stimulation and placed in their homecage. Only rats designated to receive anodal tDCS before memory recall were stimulated, and all of the other rats received sham stimulation. After the stimulation period, animals were unwrapped and placed into the same arena as the previous 2 days and allowed to explore the arena for 3 minutes. During this phase, one of the objects was randomly replaced with a different object that the rodent had not been previously exposed to. The different object was placed and rotated between animals. After the three minute exploration, the rodent was then placed into the PAT lit room chamber facing away from the gate and allowed to acclimate for 30 seconds. The gate separating the light room from the dark room was then lifted and the animal was again given the opportunity to cross into the dark room for a period of 10 minutes (600 seconds). After the animal either crossed over to the dark room or the 10 minute maximum time was reached, the animal was removed from the chamber and immediately euthanized by decapitation for brain tissue collection.

Tissue handling

Tissue preparation followed procedures described previously (Stafford et al., 2018). Briefly, hippocampal tissue from each rat was collected, frozen and stored at -80°C. The hippocampal tissues were prepared following the Syn-PER protein extraction method described by the manufacturer (ThermoFisher Scientific, Waltham, MA, USA), which yielded two protein fractions: cytosolic and synaptic fraction. The concentration of the synaptic proteins (synaptoneurosomes) was assessed for each sample in duplicates, using the bicinchoninic acid assay (ThermoFisher Scientific, Waltham, MA, USA) according to manufacturer's instructions.

Proteomic sample preparation

Synaptoneurosome isolations (15µL) were suspended in 15µL of 0.2% Rapigest surfactant (Waters, Milford, MA, USA) in 50mM ammonium bicarbonate supplemented with MS-SAFE protease/phosphatase inhibitor cocktail (Sigma-Aldrich, St. Louis, MO, USA). Protein samples were reduced with dithiothreitol (5mM final concentration, Sigma-Aldrich) at 95°C for 5 minutes. Samples were cooled and cysteines were alkylated with iodoacetamide (15mM final concentration, Sigma-Aldrich) at ambient temperature for 30 minutes in the dark, followed by the protein digestion with 800ng of sequencing grade modified trysin/Lys-C (Promega Corporation, Madison, WI, USA) at 37°C overnight with gentle shaking. Neat formic acid (Pierce, Thermo Fisher Scientific, Waltham, MA, USA) was added to each sample (50% v/v) and samples were returned to 37°C for 30 minutes. Precipitated Rapigest was removed by removing the supernatant following centrifugation at 30,000 x g for 15 minutes. Centrifugation was repeated until no precipitate remained. Samples were dried in a speed vac and resuspended in 2% acetonitrile: 0.03% trifluoroacetic acid (TFA, aq, LC loading buffer). The 280nm absorbance was used to estimate peptide concentration (Nanodrop, Wilmington, DE, USA) and samples were diluted to 0.5µg/µL in LC loading buffer.

Bottom-up liquid chromatography mass spectrometry (LC-MS/MS)

All separations were performed on a Dionex Ultimate 3000 RSLCnano liquid chromatography system (Thermo Fisher Scientific). Briefly, digested peptides (1µg) were preconcentrated on a 5µ, 100Å, 300µm x 5mm C18 PepMap 100 trap column (Thermo Fisher Scientific) using LC loading buffer under isocratic conditions at 5µL·min-1 for 7.5 minutes. Peptides were reversed-phase separated on an Easy-Spray PepMap 3µm, 100Å, 75µm x 15cm column at 300nL·min-1. Mobile phases were 0.1% formic acid (aq, A) and 0.1% formic acid in acetonitrile (B, Optima MS Grade, Thermo Fisher Scientific). Analytical separations were conducted over 180 minutes at 3% B for 10 minutes, 30% B for 152 minutes, 40% B at

157 minutes followed by a 10 minute wash at 90% B and a 10 minute equilibration at 3% B. Eluted peptides were introduced into an Orbitrap Fusion Lumos mass spectrometer equipped with Easy-Spray source operated at 2.2kV (Thermo Fisher Scientific). MS^1 scans were acquired at 120,000 resolution across 375-2000m/z utilizing the Easy-IC reagent (fluoranthene) for internal mass calibration. Precursors were selected based on a $MS^{(n-1)}$ scans and isolated for data dependent MS^n scans in the quadrapole operated with 1.2m/z isolation window. Fragments were generated by collision induced dissociation (CID) with a 10ms activation time and a 35% normalized collision energy for +2-+7 precursor charges states in the ion trap utilizing all available parallelizable time over 2 second cycles. Dynamic exclusion for MS^n scans was set at a ±10ppm mass tolerance with exclusion occurring after 1 time for 15 seconds.

Proteomic data processing

Proteomic data was searched using the Proteome Discoverer software suite (v. 2.2) equipped with the Sequest HT search engine (Thermo Fisher Scientific). Briefly, tandem data was searched against the Uniprot reviewed Rattus norvegicus (as of 25Oct17) and the common Repository of Adventitious Proteins (cRAP) databases. Search parameters were as follows: MS tolerance 10ppm, an MS^n tolerance of 0.5Da, and three allowed missed tryptic cleavages. Amino acid modifications searched were carbamidomethyl of cysteine (static), oxidation of methionine (dynamic), and acetylation of the n-terminus (dynamic). Peptide spectral matches (PSM) were evaluated utilizing the Target Decoy PSM Validator with a maximum Cn of 0.05 and a decoy database search with a target false discovery rate (FDR, q value) of 0.05 (relaxed) and 0.01 (strict). FDR was estimated with 0.05 (relaxed) and 0.01 (strict) thresholds. Precursor ion label free quantitation was performed on unique and razor peptides with retention time alignment of <10 minutes, mass tolerance 10ppm, abundance based on intensity, and data normalized to total peptide amount. Normalized abundances were exported from Proteome Discoverer for further downstream analysis described below.

Data analysis and statistical methods

Behavioral data from the passive avoidance test consisted of latency variables that were analyzed by two-way repeated measures ANOVA with the Holm-Sidak post-hoc method and Cox proportional hazard regression test. A homoscedastic two-tailed Student's t-test was conducted to identify statistically differentially expressed proteins (DEPs) of normalized abundance variables between treatment groups. Principal component analysis (PCA) on the correlation matrix with the default estimation method was employed to statistically explain the structure of normalized abundance data across groups. Hierarchical clustering analysis with the distance method of Ward to calculate distances between all pairs of clusters was performed. For these data analyses, the statistical software SigmaPlot (Ver. 12.3, Systat Software, Inc.), JMP Pro (ver. 13.2, SAS Institute Inc.) and Microsoft Excel 2013 were used.

The enrichment and pathway analysis on DEPs of the normalized abundance data sets were performed with the Panther (Protein ANalysis THrough Evolutionary Relationships) Classification System (Mi et al., 2013) and the Database for Annotation, Visualization and Integrated Discovery (DAVID) Bioinformatics resources (Huang da et al., 2009). The DAVID Bioinformatics resources was also used to perform a functional annotation clustering analysis for DEPs of the normalized abundance data sets. The DEPs were also analyzed by the Ingenuity® Pathway Analysis (IPA®, Qiagen) to identify the diseases and biological functions that are associated with behaviors. The Ingenuity® Upstream Regulator analysis in IPA® was performed to identify the upstream transcriptional regulators in addition to conducting the IPA's network analysis.

Protein-protein interaction (PPI) network analysis for the organism Rattus norvegicus (network edge setting: molecular action) was conducted for DEPs by using the STRING database (Szklarczyk et al., 2017). The Markov cluster (MCL) algorithm with an inflation parameter of 3 was used if needed. Protein sequence similarity (PSS) network analysis for the organisms Rattus norvegicus was also performed. The BLASTP suite (BLASTP 2.8.0+) was used to search proteins and determine their sequence similarity. Cytoscape (version 3.7) was used to build PSS network visualization and conduct network analysis (Shannon et al., 2003). The Cytoscape plugin app ClusterONE was used to cluster with

overlapping neighborhood expansion to detect potentially overlapping protein complexes from the interaction data (Nepusz et al., 2012). Centrality measures were calculated to identify critical proteins that play a central role in mediating interactions among given proteins in PPI and PSS networks (Jeong et al., 2001; Ashtiani et al., 2018) by using CytoNCA (Wang et al., 2012). The GeneMANIA was also used to identify the function of molecules in networks (Montojo et al., 2010; Warde-Farley et al., 2010) as needed.

RESULTS

Passive avoidance test (PAT)

The PAT was utilized to examine the effect of anodal tDCS administered before memory acquisition or memory recall on cognitive performance. Two-way repeated measures ANOVA (Session x Group) was performed for PAT latency variable. A significant trial difference ($F = 25.05$, $p < 0.001$) was detected (Figure 2A). All groups resulted in statistical significance between training and testing days, confirming that the learning experience of PAT was significantly completed by all animals across treatment groups. Additionally, on the testing day, the post hoc test shows that the acquisition group significantly performed better on PAT when compared to the sham group ($p = 0.046$), but no significant difference between sham and retrieval groups was detected. However, because the two-way repeated measures ANOVA did not detect a statistical significance from the treatment group variation ($F = 1.695$, $p = 0.196$), Cox proportional hazard regression test was also conducted for PAT data on training and testing days (Figure 2B & 2C). The result first confirmed no group difference during the training day. However, on the testing day, there is a significant difference between the acquisition and sham groups indicating that brain stimulation prior to training enhances memory performance (*Chisq* $p = 0.0445$, *Risk Ratio* = 2.306331).

295 ***Overall results of hippocampal synaptic proteomics***

296 Proteomics analysis was conducted to determine the underlying effects of brain stimulation on
297 protein abundance in the rat hippocampus, an area of the brain associated with learning and memory. The
298 proteomics data were first validated by comparing the protein abundances within each group
299 (replicability; Figure 1-1) and analyzing the abundance levels of 16 proteins that are usually used as
300 internal control (Figure 1-2). All 16 proteins show no group difference between sham and acquisition
301 groups, and 15 proteins resulted in no difference between sham and retrieval groups. The abundance
302 levels of 3687 proteins were detected, but 2909 proteins were used for further analyses because 778
303 proteins contain a value of zero for the most samples (≥ 35 samples out of 42 samples; Figure 1-3). When
304 compared to the sham group, the acquisition and retrieval groups resulted in 184 and 82 significant
305 proteins, respectively ($p < 0.0500$, two-tailed test). Interestingly, 431 proteins were significantly identified
306 when the two tDCS groups were compared. Principal component analysis (PCA) showed a clear group
307 separation between sham and acquisition groups, but the retrieval group overlapped the other groups
308 (Figure 2D). The hierarchical clustering analysis resulted in the similar pattern to the PCA result (Figure
309 2E).

310

311 ***GO enrichment analysis & pathway analysis (PantherDB & DAVID Bioinformatics)***

312 Gene Ontology (GO) enrichment analysis and pathway analysis were performed to investigate the
313 effects of tDCS on synaptoneurosomes and pathways in the rat hippocampus. Using lists of significantly,
314 differentially expressed proteins between 2 groups, GO enrichment analysis was performed by using
315 PantherDB and DAVID Bioinformatics. The analysis from the comparison between sham and retrieval
316 groups resulted in only 3 cellular component (CC) and 2 pathways. The 2 pathways are TGF-beta
317 signaling pathway (P00052, *FDR q* = 0.026) and gonadotropin-releasing hormone receptor pathway
318 (P06664, *FDR q* = 0.00223). The analysis of Panther GO slim with significant genes between sham and

acquisition groups (Table 1) resulted in 12 CC, 20 biological processes (BP), 16 molecular functions (MF) and 7 pathways. The GO slim results showed that the significant genes are significantly associated with neuronal synaptic membrane and protein complex (from CC results); neuron-neuron synaptic transmission and transport (from BP results); and significantly connected to the signaling pathways of glutamate receptor and voltage-gated ion channel activities (from MF results). The results of the Panther pathways analysis include glutamate receptor pathways (P00037, P00041 & P00039) and beta-adrenergic receptor pathways (P04378 & P04377). Moreover, the Reactome pathway analysis shows that the significant genes identified from the comparison between sham and acquisition groups are significantly involved in 20 different pathways (Table 1-1). Among them, the most abundant pathways are receptor signaling, including NMDA receptor, glutamate receptor and ion channels. From the significant genes between sham and retrieval groups, however, no significant pathways and GO slim terms for BP and MF were detected. Only 3 GO slim CCs were detected and they are: cytoplasm (GO:0005737, fold change (FC): 2.39), intracellular (GO:0005622, FC: 1.71) and cell part (GO:0044464, FC: 1.68) with q values from false discovery rate analysis less than 0.05. The significant gene list identified from the comparison between the acquisition and recall groups resulted in 20 CC, 42 BP and 26 MF with a statistical significance from the false discovery rate analysis (Table 2 & Table 2-1). The CC terms identified by the GO slim analysis includes postsynaptic membrane, synapse, SNARE complex, neuron projection and protein complex ($q < 0.05$). Growth, neuron-neuron synaptic transmission, and different transports and metabolisms were detected for the BP terms ($q < 0.05$); while glutamate receptor activity, SNAP receptor activity and multiple kinase activities were identified for the MF terms ($q < 0.05$).

The functional annotation clustering analysis provided by the DAVID Bioinformatic Database resulted in 54 annotation clusters for the comparison between sham and acquisition groups. Among them, 11 annotation clusters have an enrichment score greater than 4.0 (Table 3 & Table 3-1). The functional clustering annotation terms “postsynaptic membrane” and “synapse” resulted in the highest enrichment scores (13.96 and 12.4, respectively). Moreover, the results also contain the terms regulation of excitatory

postsynaptic potential, glutamate receptor, NMDA receptor and neuronal membrane-associated guanylate-kinase-associated proteins. However, the functional annotation clustering analysis for the comparison between sham and retrieval groups did not result in any significant FDR (the lowest $q = 1.72$) with the highest enrichment score of 1.97; thus, no further analysis was considered.

Ingenuity Pathway Analysis

Ingenuity® Pathway Analysis (IPA®) was conducted to identify the diseases and biological functions that are associated with behavior. From the comparison between retrieval and sham groups, functions of locomotion ($p = 0.00028$) and working ($p = 0.00265$) were detected (Figure 3-1). More behavior-associated functional annotations were detected from the comparison between the acquisition and sham groups (Figure 3A & Figure 3-2). Interestingly, functions of memory, cognition and learning were significantly enhanced in the acquisition group while grooming, anxiety and emotional behavior were slightly, but significantly reduced. Statistically significant diseases and functions detected from the comparison between retrieval and sham groups include angiogenesis, apoptosis, necrosis, cognitive impairment and development of neurons (activation z-scores: -2.404, -2.205, -2.159, -1.941, & 1.514, respectively). tDCS before memory acquisition significantly enhanced plasticity of synapse, neurotransmission, synaptic transmission, synaptic transmission of nervous tissue, synaptic transmission of hippocampal cells, quantity of synaptic vesicles, function of neurons, branching of neurites, neuritogenesis, and long-term potentiation (activation z-scores: 2.36, 2.718, 2.701, 2.67, 2.762, 2.0, 2.0, 1.538, 1.291 & 1.259, respectively). Additionally, the acquisition group resulted in significant decreases in neurological diseases, including hyperactive disorder, seizures, movement disorder, neurodegeneration, and cognitive impairment (activation z-scores: -3.679, -2.788, -2.015, -1.125 & -1.0, respectively).

IPA® generated multiple networks (Figure 3-3). Among them, only one network (Figure 3B) identified from the analysis between retrieval and sham groups was associated with neurological and

psychological disorders. The analysis between the acquisition and sham groups resulted in 6 networks that are associated with the nervous system. When the six networks were merged into a larger network (Figure 3C), molecules associated with memory (p = 1.65E-7), learning (p = 9.69E-16) and spatial learning (p = 9.09E-7) were most prevalent. The effects of top regulators were analyzed (Figure 3-4), but nervous system-associated regulators were not detected from the analysis between retrieval and sham groups. The analysis between the acquisition and sham group identified multiple top regulators that are associated with the nervous system. The network of regulators (APOE, BDNF, GSK3B & SHANK3) targets 17 molecules in the dataset and are associated with function of neurons, memory, plasticity of synapse and synaptic transmission (consistency score: 8.731). Additionally, 2 networks including the nervous system regulator BDNF were identified and associated with synaptic transmission (total target molecule #: 5, consistency scores: -4.919 both). Top upstream regulators were also detected from the Ingenuity® Upstream Regulator analysis in IPA®. The analysis between retrieval and sham groups identified MAPT, PSEN1 and APP (p values of overlap: 6.80E-16, 7.61E-10 & 3.77E-09, respectively) as top upstream regulators. PSEN1, MAPT1, APP, and L-dopa (p values of overlap: 2.95E-13, 3.03E-12, 1.04E-08 & 1.47E-08, respectively) were detected as the top upstream regulators for the comparison between the acquisition and sham groups.

Network Analysis

Protein-protein interaction (PPI) networks were developed and analyzed to identify the effects of stimulation on protein signaling cascades. The PPI network for the statistically significant molecules detected from the retrieval compared to the sham group was not significant (average node degree: 0.53; average local clustering coefficient: 0.317; PPI enrichment p value = 0.648). However, the PPI network from the acquisition group compared to the sham group had significant interactions (average node degree: 3.06; average local clustering coefficient: 0.404; PPI enrichment p value< 1.0E-16; Figure 4A). The PPI network was further clustered by the MCL method. The MCL cluster-1 network (Figure 4B) was

393 significantly related to the glutamate receptor signaling pathway (brown colored nodes; q = 2.68E-29),
394 memory (purple colored nodes; q = 5.94E-07), learning (green colored nodes; q = 1.097E-06), cognition
395 (blue colored nodes; q = 4.98E-06), and long-term memory (yellow colored nodes; q = 0.0001). The MCL
396 cluster-2 network (Figure 4C) was significantly associated with the function of voltage-gated channel
397 activity (brown colored nodes; q = 4.03E-40). Network centralities were calculated for the MCL cluster-1
398 network to identify candidate molecules that may lethally affect to the network. Based on the subgraph
399 centrality measure, the top 5 ranked proteins are DLG4, GRIN2a, SHANK1, GRIA1 & DLG3, and the
400 expression of these proteins resulted in significant group difference between the acquisition and sham
401 groups ($p < 0.01$).

402 The BLASTP suite (BLASTP 2.8.0+) was used to search for proteins and determine their
403 sequence similarity. Protein sequence similarity (PSS) network was created by using Cytoscape, and
404 proteins were clustered based on their sequence similarity. Among the 25 clusters identified, only 9
405 clusters were statistically significant (p values for all clusters < 0.05, Figure 5). However, clusters 3, 4
406 and 6 did not reach statistical significance for the enrichment analysis (PPI enrichment p value > 0.05).
407 As shown in Figure 5, each cluster is significantly related to a specific functional enrichment annotation.
408 The clusters 1 and 5 are significantly related to glutamatergic pathways while clusters 2 and 8 are
409 associated with voltage-gated channel activities. Functional annotations of protein domain specific
410 binding and Pentraxin were significantly associated with the clusters 7 and 9, respectively. Based on the
411 results of subgraph centrality measure for the PSS network, the top 10 ranked proteins are MACF1,
412 SHANK1, ARHGEF6, DLG3, MPP2, MPP4, ARHGEF9, SHANK3, SHANK2, SHANK2 isoform 4 and
413 MAGI2. The expression of the 9 proteins (SHANK2 isoform 4 excluded) was significantly different
414 between the acquisition and sham groups ($p < 0.05$).

415

416 **DISCUSSION**

In this study, we examined whether anodal tDCS could improve performance in a learning and memory task and the underlying protein modifications in the hippocampus, a brain region important for memory acquisition and recall. We have demonstrated that the timing of anodal tDCS is critical for memory performance. Anodal tDCS only improved memory performance when brain stimulation was applied before the acquisition period of the PAT. We further investigated the regulatory mechanisms for the memory enhancing effects of tDCS. Our results indicate tDCS induces changes in hippocampal synaptoneurosomes enhancing pathways related to cognition, learning and memory. Additional analysis identified that the enhanced pathways are associated with specific receptor signaling and ion channel activity.

Our finding that anodal tDCS enhances cognitive performance when administered before memory acquisition is consistent with previous studies. A human-based study reported that tDCS enhances verbal memorization when anodal stimulation is applied during the memory encoding period (Javadi and Walsh, 2012). Another recent study shows that anodal tDCS delivered during the memory encoding period, but not the retrieval period, enhances memory (Medvedeva et al., 2019). Fertonani and colleagues (Fertonani et al., 2014) also found that the timing of stimulation in relation to a cognitive task significantly affected performance. Together, previous studies and our current work suggest that tDCS-induced memory enhancement is dependent on the timing of tDCS administration.

To understand the underlying mechanisms for anodal tDCS-induced memory enhancement, we profiled proteins in the hippocampal synaptoneurosomes and analyzed the proteomic data. Compared to the sham treatment group, there were significant differences in protein abundances for the acquisition group (184 proteins). The PCA and hierarchical clustering analysis show a clear separation in distribution for the sham and acquisition groups. Enrichment and pathway analyses for the statistically significant proteins between the sham and acquisition group show changes in hippocampal protein regulation associated with synaptic neurotransmission and transporters. Using multiple database analyses from PantherDB and David bioinformatics (Tables 1 & 3), we further identified pathways involving glutamate

receptor and ion channel signaling. Glutamate receptors and ion channels regulate neuronal activity and synaptic plasticity, which underlie neurological processes of learning and memory (Gasque et al., 2006; Voglis and Tavernarakis, 2006; Gecz, 2010; Queenan et al., 2017; Foster et al., 2018). Although the underlying mechanisms of tDCS on learning and memory remain under investigation, our data show that anodal tDCS applied before the memory acquisition period modifies the regulation of hippocampal glutamate signaling and ion channel activity ultimately resulting in enhanced memory performance in rats.

We used IPA to understand hippocampal biological functions associated with learning and memory. Similar to the enrichment and pathway analysis results, the comparison between the acquisition and sham groups identified significant enhancements of memory, cognition, and learning while negative behaviors, such as anxiety, were significantly reduced. Our data show that anodal tDCS applied before the acquisition period modifies synaptic proteomic regulation in a manner associated with multiple electrophysiological and molecular pathways such as neuritogenesis, long-term potentiation (LTP), branching of neurites and synaptic transmission, which consequently enhance learning and memory. There is evidence that these pathways possibly explain the beneficial effects of tDCS on cognition. For example, tDCS has been reported to modulate LTP, which is well known to enhance cognition (Ranieri et al., 2012). Additionally, the networks developed by IPA contain many molecules that have been known to be associated with learning and memory. APOE, BDNF, GSK3B & SHANK3 were identified as candidate regulators of the network to control memory and synaptic plasticity. PSEN1, MAPT1, APP, and L-dopa were identified as upstream regulators for significant proteins detected from the comparison between sham and acquisition groups. Most of these candidate regulators have been reported to be associated with cognition: APOE (Risacher et al., 2015; Sinclair et al., 2015), BDNF (Poo, 2001), PSEN1 (Kennard and Harrison, 2014), APP (Tamayev and D'Adamio, 2012) and L-DOPA (Murer and Moratalla, 2011). A recent study shows that tDCS induces BDNF expression and consequently enhances memory (Cocco et al., 2018). Based on the results of the Ingenuity upstream regulator analysis in IPA, our study is

467 the first to suggest the following potential candidate regulators for anodal tDCS effects on learning and
468 memory: GSK3b, SHANK3 and MAPT1. Most research on the role SHANK3 in the brain is related to
469 autism (Yi et al., 2016). Recently, Duffney and colleagues (Duffney et al., 2013) showed that SHANK3 is
470 associated with NMDA receptor function, suggesting a potential role for SHANK3 in learning and
471 memory. Currently, there are no published reports linking GSK3b with tDCS-induced learning and
472 memory, but a recent study reported that GSK3b is associated with Alzheimer's disease (Jayapalan and
473 Natarajan, 2013). We cannot find any research that investigates roles of MAPT1 in learning and memory,
474 but there is evidence that a MAPT mutation may be indirectly associated with cognitive dysfunction
475 observed in dementia (Iyer et al., 2013). More work is needed to elucidate the roles of these novel
476 candidate molecules in learning and memory.

477 To identify significant protein networks for tDCS-induced effects on proteomic modifications of
478 the hippocampal synapse, we conducted network analysis. The PPI network for the acquisition group
479 compared to sham group is significantly associated with learning, memory, cognition, long-term memory,
480 and glutamate receptor signaling pathways. Significant glutamate signaling pathways and ion channel
481 activity were also identified from the PSS network. A relationship between ion channel activity and
482 memory performance has been previously reported (Cavallaro, 2004) and it showed higher ion channel
483 activity in animals is significantly associated with better memory performance as measured by the passive
484 avoidance test. Glutamate receptor signaling pathways are also known to be dynamically regulated during
485 learning and memory (Tronson and Taylor, 2007; Poo et al., 2016; Foster et al., 2018). Our studies have
486 identified significant glutamate signaling and channel activity for the acquisition and sham group
487 comparison using multiple analyses including enrichment and pathway analyses, IPA and PPI and PSS
488 networks providing additional evidence for the mechanism of tDCS effects on hippocampal
489 synaptoneurosomes. Therefore, our data suggest that anodal tDCS applied before the acquisition period
490 modifies glutamate signaling and ion channel activity and consequently enhances memory performance.
491 Our results identifying glutamatergic signaling as a mechanism for tDCS-induced effects on learning are

492 supported by previous reports (Rossini et al., 2015; Giordano et al., 2017; Stafford et al., 2018). Our work
493 is the first to use proteomics to suggest possible molecular effects associated with tDCS-enhancing
494 memory acquisition by modifying glutamate signaling and ion channel activity pathways in rat
495 hippocampal synaptoneurosomes.

496 From the PPI and PSS networks, we identified key molecules that lethally affect the protein
497 networks. Key molecules in the networks identified by subgraph centrality measure include SHANK,
498 DLG, GRIN and GRIA proteins. Although future studies are needed to investigate the effects of these key
499 players in the network, our work supports possible roles of these proteins in learning and memory. The
500 function of glutamate receptor (Grin2a and Gria1) in learning and memory is well understood.
501 Additionally, recent studies suggest SHANK may mediate the activity of glutamate receptors in neurons
502 (Bertaso et al., 2010; Ha et al., 2018) and may play a role in synapse formation and plasticity (Kilinc,
503 2018). SHANK was also identified as one of the regulators in the network from the IPA suggesting that
504 anodal tDCS modulates SHANK and subsequently affects synaptic plasticity and transmission in
505 hippocampal neurons. Additionally, SHANK and DLG proteins were also identified as critical molecules
506 in the PSS network.

507 Bioinformatics and network analyses were completed for the comparisons of the retrieval group
508 to the sham and acquisition group even through the behavioral data were not significant. Compared to the
509 sham treatment group, there were significant differences in protein abundance for the retrieval group (82
510 proteins) Furthermore, the candidate regulators suggested from the Ingenuity upstream regulator analysis
511 in IPA for the comparison between the sham and acquisition group (see above) did not result in a
512 statistically significant difference. Additionally, the clustering analyses did not show a clear separation
513 between the retrieval group and the sham and acquisition groups. Comparison of the acquisition group to
514 the retrieval group using enrichment and pathway analyses, generated significant effects of hippocampal
515 protein regulation of glutamate receptor pathways and ion channel pathways. Unique pathways identified
516 for the acquisition and retrieval group comparison include pyrophosphatase activity and SNAP receptor

activity. Many similar pathways were identified from the acquisition and sham versus the acquisition and retrieval group comparisons (see Tables 1 & 2), suggesting similarity between the sham and retrieval groups. More time post stimulation may be needed for the molecular modifications in the retrieval group to show a clear separation from the sham group.

In summary, we investigated whether anodal tDCS could affect memory acquisition, recall, or both, and the underlying molecular modifications in hippocampal synaptoneurosomes. We found that anodal tDCS administered before acquisition significantly enhanced memory performance potentially by enhancing the abundance of proteins associated with glutamate signaling and ion channel activity in hippocampal synapses. Our results also suggest potential molecular targets for the effects of anodal tDCS on memory performance. Our work contributes to the understanding of the regulatory molecular mechanisms of tDCS-induced memory enhancements. However, because the focus of our study is to observe molecular differences in hippocampal synapses and correlate proteomic changes with rodent cognitive performance, we should point out that our data do not report any cause-and-effect relationship between proteomic modifications, tDCS, and cognitive performance. Thus, future studies are needed to investigate the causal effects of the proteins identified from our study. Increased understanding of the mechanisms for the effects of tDCS on memory enhancement will facilitate future applications of brain stimulation.

Author contributions

SHJ-Designed research, analyzed data, interpreted data, wrote the paper; CHS-Interpreted data, obtained funding for research, wrote the paper; RM-performed research; NB-performed research; SH-performed research; JM-performed research, interpreted data;; RJ-Designed research, obtained funding for research, edited the paper.

Funding

This work was supported by the Air Force Office of Scientific Research (AFOSR grant numbers 13RH14COR and 16RHCOR362) and has been approved for public release (Distribution A: Approved for public release. 88ABW Cleared 05/July/2019; 88ABW-2019-3239).

Data availability

Proteomics data are provided as a Figure 1-3.

549 **REFERENCES**

550 Alonzo A, Brassil J, Taylor JL, Martin D, Loo CK (2012) Daily transcranial direct current stimulation
551 (tDCS) leads to greater increases in cortical excitability than second daily transcranial direct
552 current stimulation. Brain Stimul 5:208-213.

553 Ashtiani M, Salehzadeh-Yazdi A, Razaghi-Moghadam Z, Hennig H, Wolkenhauer O, Mirzaie M, Jafari
554 M (2018) A systematic survey of centrality measures for protein-protein interaction networks.
555 BMC Syst Biol 12:80.

556 Bailey NW, Thomson RH, Hoy KE, Hernandez-Pavon JC, Fitzgerald PB (2016) TDCS increases cortical
557 excitability: Direct evidence from TMS-EEG. Cortex 74:320-322.

558 Bertaso F, Roussignol G, Worley P, Bockaert J, Fagni L, Ango F (2010) Homer1a-dependent crosstalk
559 between NMDA and metabotropic glutamate receptors in mouse neurons. PLoS One 5:e9755.

560 Bogdanov M, Schwabe L (2016) Transcranial Stimulation of the Dorsolateral Prefrontal Cortex Prevents
561 Stress-Induced Working Memory Deficits. J Neurosci 36:1429-1437.

562 Boggio PS, Ferrucci R, Rigonatti SP, Covre P, Nitsche M, Pascual-Leone A, Fregni F (2006) Effects of
563 transcranial direct current stimulation on working memory in patients with Parkinson's disease. J
564 Neurol Sci 249:31-38.

565 Cattaneo Z, Pisoni A, Papagno C (2011) Transcranial direct current stimulation over Broca's region
566 improves phonemic and semantic fluency in healthy individuals. Neuroscience 183:64-70.

567 Cavallaro S (2004) DNA microarrays and animal models of learning and memory. Int Rev Neurobiol
568 60:97-133.

569 Cocco S, Podda MV, Grassi C (2018) Role of BDNF Signaling in Memory Enhancement Induced by
570 Transcranial Direct Current Stimulation. Front Neurosci 12:427.

571 Duffney LJ, Wei J, Cheng J, Liu W, Smith KR, Kittler JT, Yan Z (2013) Shank3 deficiency induces
572 NMDA receptor hypofunction via an actin-dependent mechanism. J Neurosci 33:15767-15778.

573 Fertonani A, Brambilla M, Cotelli M, Miniussi C (2014) The timing of cognitive plasticity in
574 physiological aging: a tDCS study of naming. Front Aging Neurosci 6:131.
575 Floel A, Suttorp W, Kohl O, Kurten J, Lohmann H, Breitenstein C, Knecht S (2012) Non-invasive brain
576 stimulation improves object-location learning in the elderly. Neurobiol Aging 33:1682-1689.
577 Foster WJ, Taylor HBC, Padamsey Z, Jeans AF, Galione A, Emptage NJ (2018) Hippocampal mGluR1-
578 dependent long-term potentiation requires NAADP-mediated acidic store Ca(2+) signaling. Sci
579 Signal 11.
580 Gasque G, Labarca P, Delgado R, Darszon A (2006) Bridging behavior and physiology: ion-channel
581 perspective on mushroom body-dependent olfactory learning and memory in Drosophila. J Cell
582 Physiol 209:1046-1053.
583 Gecz J (2010) Glutamate receptors and learning and memory. Nat Genet 42:925-926.
584 Giordano J, Bikson M, Kappenman ES, Clark VP, Coslett HB, Hamblin MR, Hamilton R, Jankord R,
585 Kozumbo WJ, McKinley RA, Nitsche MA, Reilly JP, Richardson J, Wurzman R, Calabrese E
586 (2017) Mechanisms and Effects of Transcranial Direct Current Stimulation. Dose Response
587 15:1559325816685467.
588 Goder R, Baier PC, Beith B, Baecker C, Seeck-Hirschner M, Junghanns K, Marshall L (2013) Effects of
589 transcranial direct current stimulation during sleep on memory performance in patients with
590 schizophrenia. Schizophr Res 144:153-154.
591 Ha HTT, Leal-Ortiz S, Lalwani K, Kiyonaka S, Hamachi I, Mysore SP, Montgomery JM, Garner CC,
592 Huguenard JR, Kim SA (2018) Shank and Zinc Mediate an AMPA Receptor Subunit Switch in
593 Developing Neurons. Front Mol Neurosci 11:405.
594 Hill AT, Rogasch NC, Fitzgerald PB, Hoy KE (2018) Impact of concurrent task performance on
595 transcranial direct current stimulation (tDCS)-Induced changes in cortical physiology and
596 working memory. Cortex 113:37-57.
597 Holland R, Leff AP, Josephs O, Galea JM, Desikan M, Price CJ, Rothwell JC, Crinion J (2011) Speech
598 facilitation by left inferior frontal cortex stimulation. Curr Biol 21:1403-1407.

599 Holmes B, Jung SH, Lu J, Wagner JA, Rubbi L, Pellegrini M, Jankord R (2016) Transcriptomic
600 Modification in the Cerebral Cortex following Noninvasive Brain Stimulation: RNA-Sequencing
601 Approach. Neural Plast 2016:5942980.
602 Hoy KE, Emonson MR, Arnold SL, Thomson RH, Daskalakis ZJ, Fitzgerald PB (2013) Testing the
603 limits: Investigating the effect of tDCS dose on working memory enhancement in healthy
604 controls. Neuropsychologia 51:1777-1784.
605 Huang da W, Sherman BT, Lempicki RA (2009) Bioinformatics enrichment tools: paths toward the
606 comprehensive functional analysis of large gene lists. Nucleic Acids Res 37:1-13.
607 Iyer A, Lapointe NE, Zielke K, Berdynski M, Guzman E, Barczak A, Chodakowska-Zebrowska M,
608 Barcikowska M, Feinstein S, Zekanowski C (2013) A novel MAPT mutation, G55R, in a
609 frontotemporal dementia patient leads to altered Tau function. PLoS One 8:e76409.
610 Jacobson L, Goren N, Lavidor M, Levy DA (2012) Oppositional transcranial direct current stimulation
611 (tDCS) of parietal substrates of attention during encoding modulates episodic memory. Brain Res
612 1439:66-72.
613 Javadi AH, Walsh V (2012) Transcranial direct current stimulation (tDCS) of the left dorsolateral
614 prefrontal cortex modulates declarative memory. Brain Stimul 5:231-241.
615 Javadi AH, Cheng P (2013) Transcranial direct current stimulation (tDCS) enhances reconsolidation of
616 long-term memory. Brain Stimul 6:668-674.
617 Jayapalan S, Natarajan J (2013) The role of CDK5 and GSK3B kinases in hyperphosphorylation of
618 microtubule associated protein tau (MAPT) in Alzheimer's disease. Bioinformation 9:1023-1030.
619 Jeong H, Mason SP, Barabasi AL, Oltvai ZN (2001) Lethality and centrality in protein networks. Nature
620 411:41-42.
621 Kennard JA, Harrison FE (2014) Intravenous ascorbate improves spatial memory in middle-aged
622 APP/PSEN1 and wild type mice. Behav Brain Res 264:34-42.
623 Kilinc D (2018) The Emerging Role of Mechanics in Synapse Formation and Plasticity. Front Cell
624 Neurosci 12:483.

625 Kim MS, Koo H, Han SW, Paulus W, Nitsche MA, Kim YH, Yoon JA, Shin YI (2017) Repeated anodal
626 transcranial direct current stimulation induces neural plasticity-associated gene expression in the
627 rat cortex and hippocampus. Restor Neurol Neurosci 35:137-146.
628 Ladenbauer J, Ladenbauer J, Kulzow N, de Boor R, Avramova E, Grittner U, Floel A (2017) Promoting
629 Sleep Oscillations and Their Functional Coupling by Transcranial Stimulation Enhances Memory
630 Consolidation in Mild Cognitive Impairment. J Neurosci 37:7111-7124.
631 Marshall L, Molle M, Hallschmid M, Born J (2004) Transcranial direct current stimulation during sleep
632 improves declarative memory. J Neurosci 24:9985-9992.
633 Martin DM, Liu R, Alonzo A, Green M, Loo CK (2014) Use of transcranial direct current stimulation
634 (tDCS) to enhance cognitive training: effect of timing of stimulation. Exp Brain Res 232:3345-
635 3351.
636 Medvedeva A, Materassi M, Neacsu V, Beresford-Webb J, Hussin A, Khan N, Newton F, Galli G (2019)
637 Effects of Anodal Transcranial Direct Current Stimulation Over the Ventrolateral Prefrontal
638 Cortex on Episodic Memory Formation and Retrieval. Cereb Cortex 29:657-665.
639 Mi H, Muruganujan A, Thomas PD (2013) PANTHER in 2013: modeling the evolution of gene function,
640 and other gene attributes, in the context of phylogenetic trees. Nucleic Acids Res 41:D377-386.
641 Montojo J, Zuberi K, Rodriguez H, Kazi F, Wright G, Donaldson SL, Morris Q, Bader GD (2010)
642 GeneMANIA Cytoscape plugin: fast gene function predictions on the desktop. Bioinformatics
643 26:2927-2928.
644 Murer MG, Moratalla R (2011) Striatal Signaling in L-DOPA-Induced Dyskinesia: Common
645 Mechanisms with Drug Abuse and Long Term Memory Involving D1 Dopamine Receptor
646 Stimulation. Front Neuroanat 5:51.
647 Nepusz T, Yu H, Paccanaro A (2012) Detecting overlapping protein complexes in protein-protein
648 interaction networks. Nat Methods 9:471-472.

649 Podda MV, Cocco S, Mastrodonato A, Fusco S, Leone L, Barbati SA, Colussi C, Ripoli C, Grassi C
650 (2016) Anodal transcranial direct current stimulation boosts synaptic plasticity and memory in
651 mice via epigenetic regulation of Bdnf expression. Sci Rep 6:22180.
652 Poo MM (2001) Neurotrophins as synaptic modulators. Nat Rev Neurosci 2:24-32.
653 Poo MM, Pignatelli M, Ryan TJ, Tonegawa S, Bonhoeffer T, Martin KC, Rudenko A, Tsai LH, Tsien
654 RW, Fishell G, Mullins C, Goncalves JT, Shtrahman M, Johnston ST, Gage FH, Dan Y, Long J,
655 Buzsaki G, Stevens C (2016) What is memory? The present state of the engram. BMC Biol
656 14:40.
657 Queenan BN, Ryan TJ, Gazzaniga MS, Gallistel CR (2017) On the research of time past: the hunt for the
658 substrate of memory. Ann N Y Acad Sci 1396:108-125.
659 Ranieri F, Podda MV, Riccardi E, Frisullo G, Dileone M, Profice P, Pilato F, Di Lazzaro V, Grassi C
660 (2012) Modulation of LTP at rat hippocampal CA3-CA1 synapses by direct current stimulation. J
661 Neurophysiol 107:1868-1880.
662 Risacher SL, Kim S, Nho K, Foroud T, Shen L, Petersen RC, Jack CR, Jr., Beckett LA, Aisen PS,
663 Koeppe RA, Jagust WJ, Shaw LM, Trojanowski JQ, Weiner MW, Saykin AJ, Alzheimer's
664 Disease Neuroimaging I (2015) APOE effect on Alzheimer's disease biomarkers in older adults
665 with significant memory concern. Alzheimers Dement 11:1417-1429.
666 Rohan JG, Carhuatanta KA, McInturf SM, Miklasevich MK, Jankord R (2015) Modulating Hippocampal
667 Plasticity with In Vivo Brain Stimulation. The Journal of neuroscience : the official journal of the
668 Society for Neuroscience 35:12824-12832.
669 Romero Lauro LJ, Rosanova M, Mattavelli G, Convento S, Pisoni A, Opitz A, Bolognini N, Vallar G
670 (2014) TDCS increases cortical excitability: direct evidence from TMS-EEG. Cortex 58:99-111.
671 Rossini PM et al. (2015) Non-invasive electrical and magnetic stimulation of the brain, spinal cord, roots
672 and peripheral nerves: Basic principles and procedures for routine clinical and research
673 application. An updated report from an I.F.C.N. Committee. Clin Neurophysiol 126:1071-1107.

674 Shannon P, Markiel A, Ozier O, Baliga NS, Wang JT, Ramage D, Amin N, Schwikowski B, Ideker T
675 (2003) Cytoscape: a software environment for integrated models of biomolecular interaction
676 networks. Genome Res 13:2498-2504.
677 Sinclair LI, Button KS, Munafo MR, Day IN, Lewis G (2015) Possible Association of APOE Genotype
678 with Working Memory in Young Adults. PLoS One 10:e0135894.
679 Stafford J, Brownlow ML, Qualley A, Jankord R (2018) AMPA receptor translocation and
680 phosphorylation are induced by transcranial direct current stimulation in rats. Neurobiol Learn
681 Mem 150:36-41.
682 Stagg CJ, Nitsche MA (2011) Physiological basis of transcranial direct current stimulation. Neuroscientist
683 17:37-53.
684 Szklarczyk D, Morris JH, Cook H, Kuhn M, Wyder S, Simonovic M, Santos A, Doncheva NT, Roth A,
685 Bork P, Jensen LJ, von Mering C (2017) The STRING database in 2017: quality-controlled
686 protein-protein association networks, made broadly accessible. Nucleic Acids Res 45:D362-
687 D368.
688 Tamayev R, D'Adamio L (2012) Memory deficits of British dementia knock-in mice are prevented by
689 Abeta-precursor protein haploinsufficiency. J Neurosci 32:5481-5485.
690 Tronson NC, Taylor JR (2007) Molecular mechanisms of memory reconsolidation. Nat Rev Neurosci
691 8:262-275.
692 Voglis G, Tavernarakis N (2006) The role of synaptic ion channels in synaptic plasticity. EMBO Rep
693 7:1104-1110.
694 Wang J, Li M, Wang H, Pan Y (2012) Identification of essential proteins based on edge clustering
695 coefficient. IEEE/ACM Trans Comput Biol Bioinform 9:1070-1080.
696 Warde-Farley D, Donaldson SL, Comes O, Zuberi K, Badrawi R, Chao P, Franz M, Grouios C, Kazi F,
697 Lopes CT, Maitland A, Mostafavi S, Montojo J, Shao Q, Wright G, Bader GD, Morris Q (2010)
698 The GeneMANIA prediction server: biological network integration for gene prioritization and
699 predicting gene function. Nucleic Acids Res 38:W214-220.

700 Yi F, Danko T, Botelho SC, Patzke C, Pak C, Wernig M, Sudhof TC (2016) Autism-associated SHANK3
701 haploinsufficiency causes Ih channelopathy in human neurons. Science 352:aaf2669.
702 Yu TH, Wu YJ, Chien ME, Hsu KS (2019) Transcranial direct current stimulation induces hippocampal
703 metaplasticity mediated by brain-derived neurotrophic factor. Neuropharmacology 144:358-367.

704

FIGURE LEGENDS

Figure 1. Overall Research Design

* Before rodents were exposed to the passive avoidance memory task, they were freely exposed to open field for 5 minutes (the acquisition day) and 3 minutes (the training and testing days) for exploration with familiar and novel objects similar to the novel object recognition task. Proteomic abundance data were first analyzed for the replicability within each group (Figure 1-1), and the abundance of 16 internal control proteins were compared between the groups (Figure 1-2). Proteomic data analyzed for this manuscript were provided as an Excel file (Figure 1-3).

Figure 1-1. Replicability of Proteomic Abundance Data within Each Group.

The abundance values within each group were analyzed and the lowest r2 for the sham, acquisition and retrieval groups were 0.89, 0.91 and 0.72, respectively.

Figure 1-2. Abundance Comparison of 16 Internal Control Proteins between Groups.

None of all 16 internal control proteins resulted in no significant difference between acquisition and sham groups. The comparison between retrieval and sham groups, one internal control protein (*Aldoa*) showed a significant group difference. The abundance data of three internal control proteins (*Aldoa*, *Gdir1* & *Pgk1*) resulted in a significant group difference between acquisition and retrieval groups.

Figure 1-3. Proteomics data.

Proteomics data analyzed for this manuscript were provided as an Excel file.

Figure 2. Behavioral Data Analysis

(A) Analysis of passive avoidance data. 2-way RM ANOVA detected a significant difference in the latency of all groups between the training and testing days. During the testing day, a statistical significance was detected between sham and acquisition groups. # Habituation data was collected from only 8 animals per group. * and ** indicate statistical significance ($p < 0.05$

& 0.001, respectively). (B) Cox proportional hazard regression analysis for PAT data on training day. No statistical group separation was detected. (C) Cox proportional hazard regression analysis for PAT data on testing day. A significant group difference was detected (Log-Rank X^2 = 7.0919, df = 2, p = 00288) (D) Principal component analysis with proteomics data show the distribution of each samples across the groups. (E) Hierarchical clustering analysis with proteomics data show the distribution of each sample across the groups. Red, green and blue boxes represent sham, retrieval and acquisition samples. Protein IDs in the 1st hierarchical clustering group, from left to right, are KDELC2, EXOC6, UFL1, CDH8, ARHGAP27, BLNK, MPPED2, GFM1, FNTB, WASH, PDE4DIP, TUBA4A, ACVR1B, PRKAR1B, RBMX2, ZFYVE27, CAPN5, PSME1, KCNA6, LLGL1, JAM3, CD151, S1PR5, and GPSM1. The hierarchical clustering group 2 includes, from left to right, LHX1, GUCY1A2, STX8, CSAD, USP19, FTSJD2, DNAH7, LOC362863, RAB9A, GSTZ1, PDIA4, RPH3AL, LRFN1, STK39, CCDC116, LOC100911646, GLS, PYROXD2, LOC100911456, AOC3, MYO1C, and ILK. For the cluster group 3, protein IDs are INHBA, EIF3J, SLC20A1, ZRANB2, CCDC127, FAM195B, GLDN, FHIT, PNPO, PGP, TUBA1C, ACBD6, MCCC1, NOP58, ITGAD, RPL27, ABCF1, WDR81, and COTL1. The cluster group 4 contains proteins named as, from left to right, CACNA1D, GHITM2, SCFD1, PTP4A2, ZW10, GCLM, APMAP, CRP, SRP54, PTPRN2, SRP542, ADCY6, CAR3, COL3A1, IP6K1, GOLPH31, SLC27A1, RILPL1, PFKFB1, PSMA2, and ICOS. Proteins from the cluster group 5 are GALE, EQTN, CLUL1, GABRB2, MRPS25, MRAS, SCYL1, OXCT1, FAM194A, FAM213B, LAMP5, SNX1, CNIH2, GHITM, SLC29A3, and AK6. Proteins in the cluster group 6 are MARK2, HOMER3, GPHN, RAB3GAP2, RBP1, PALMD, MCCC2, ARHGEF11, and LRRC57. For clear figure, see the Figure 2-1

Figure 2-1. Hierarchical clustering analysis with proteomics data show the distribution of each sample across the groups.

Figure 3. IPA Results

(A) Behavior-associated functional annotation detected from the comparison between the acquisition and sham groups. (B) Network-1 detected from the comparison between the retrieval and sham groups. (C) Six networks that were associated with the nervous system were merged in to a network. Nodes that did not pass cutoff in dataset, not in overlaid dataset, and not connected to any other nodes were excluded from the network. Pink-outlined molecules are associated with cognition (p = 1.81E-3). Molecule Activity Predictor (MAP) was also overlaid to predict the upstream and downstream effects of activation or inhibition on other molecules. For all IPA data, see the Extended Figures 3-1 to 3-4.

Figure 3-1. IPA Diseases or Functions Annotation for the comparison between Retrieval and Sham groups

Figure 3-2. IPA Diseases or Functions Annotation for the comparison between Acquisition and Sham groups

Figure 3-3. Lists of IPA-generated Networks for the Comparisons between Retrieval and Sham Groups and between Acquisition and Sham Groups

Figure 3-4. Top Regulators from the IPA Upstream Analysis for the Comparisons between Retrieval and Sham Groups and between Acquisition and Sham Groups.

Figure 4. Protein-Protein Interaction Network Analysis

(A) Protein-protein interaction (PPI) network for the significant molecules from the Acquisition-and-Sham comparison. Nodes were colored for functions of glutamatergic synapse (blue), metabolic pathways (yellow), dopaminergic synapse (green), long-term potentiation (red) and cholinergic synapse (pink). Disconnected nodes were excluded. (B) The 1st cluster network of Markov clustering (MCL) algorithm. (C) The 2nd cluster network of MCL algorithm.

Figure 5. Protein Sequence Similarity Network Analysis.

783 The BLASTP suite (BLASTP 2.8.0+) was used to search proteins and determine their sequence
784 similarity. Protein sequence similarity (PSS) network was created by using Cytoscape. The PSS
785 network was clustered by using ClusterONE, and 9 clusters were significantly identified. The
786 edges were weighted by their sequence similarity and the enrichment analysis was performed for
787 each of the 9 clusters to identify specific signaling pathways of the clusters.
788

TABLE LEGENDS

Table 1-1. Results of Reactome Pathway Analysis for the Comparison Between Sham and Acquisition Groups

Table 2-1. Results of Gene Ontology Slim Analysis for the Comparison Between Acquisition and Retrieval Groups

Table 3-1. Results of Functional Clustering Annotation Analysis for the Comparison Between Sham and Acquisition Groups

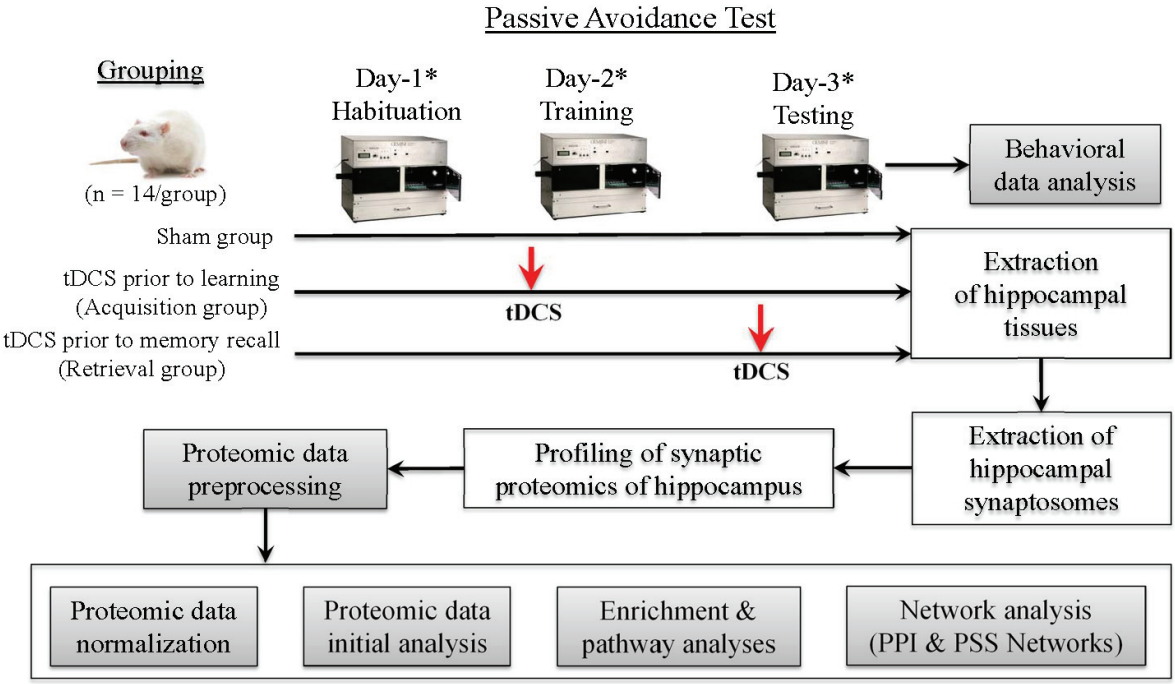

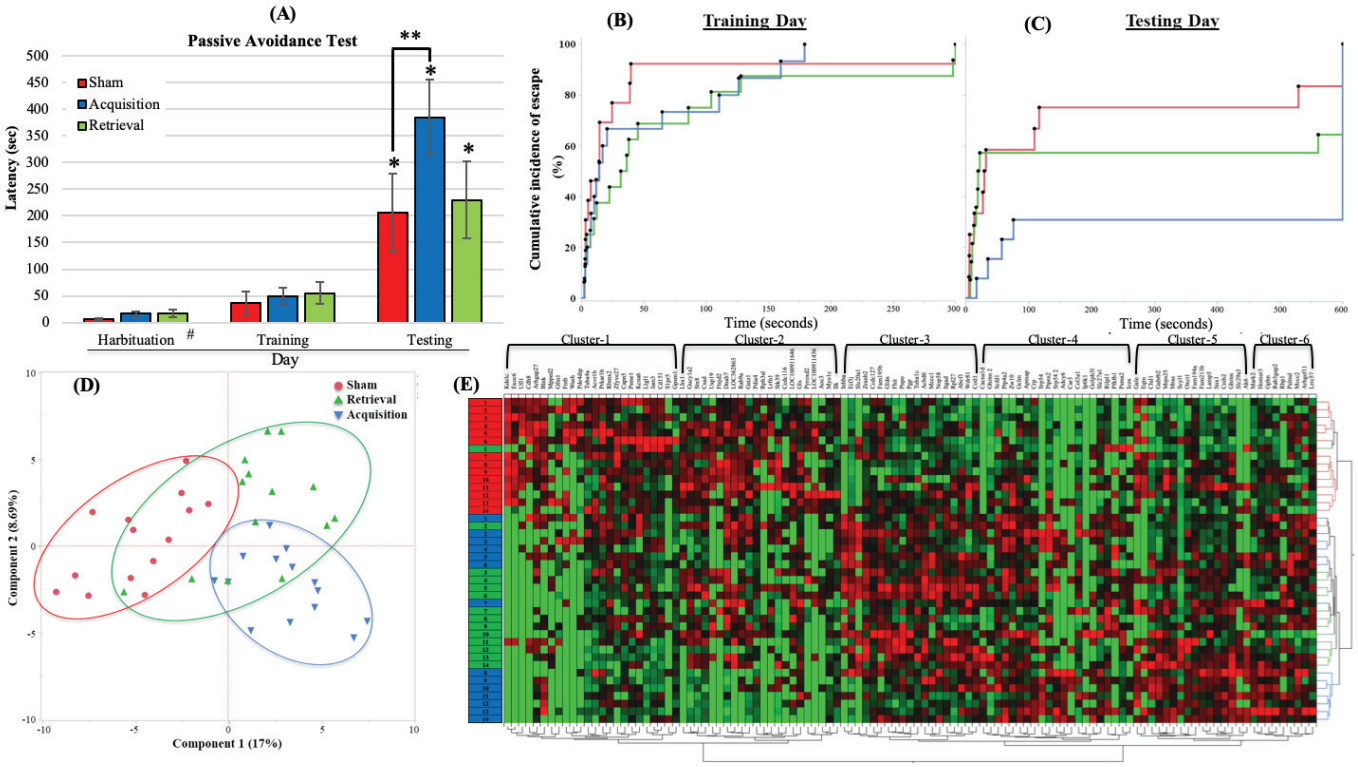

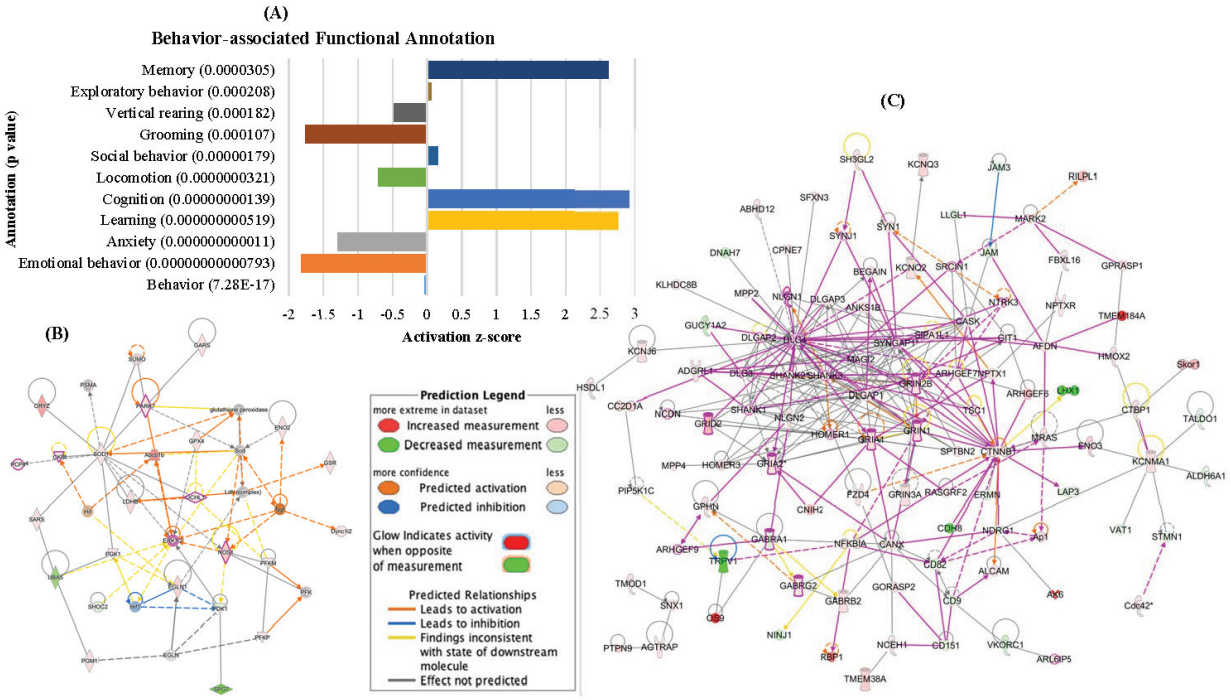

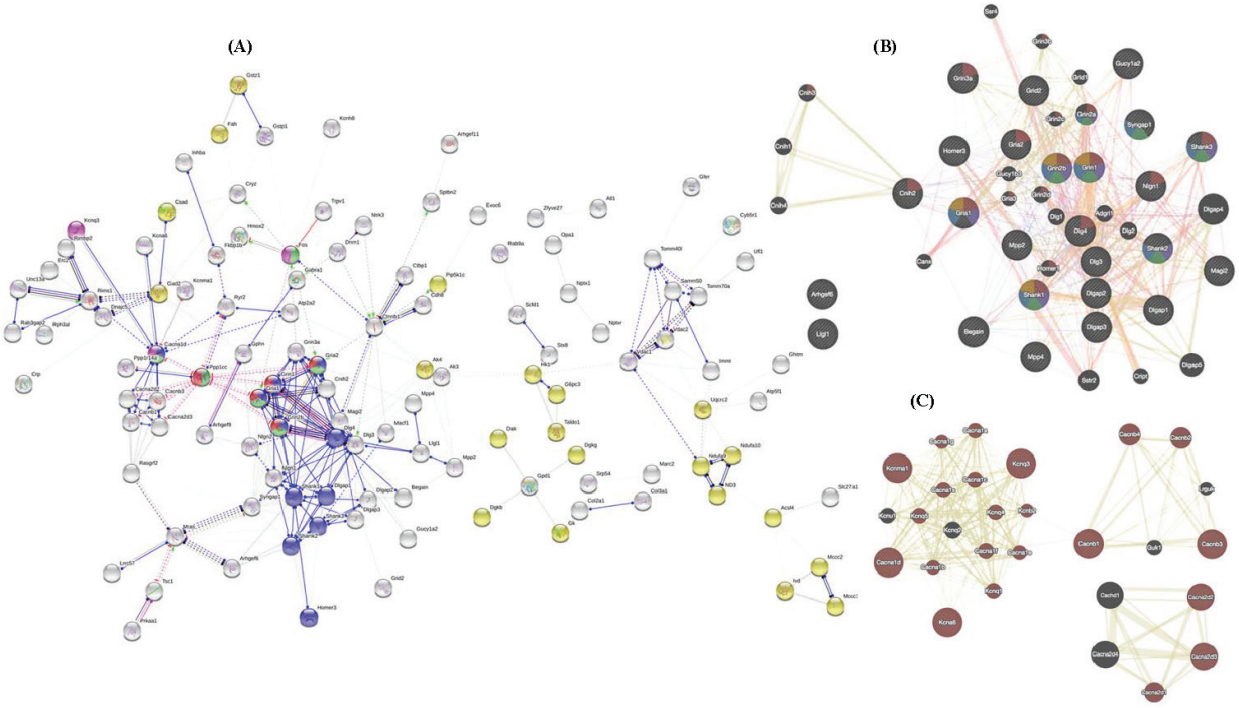

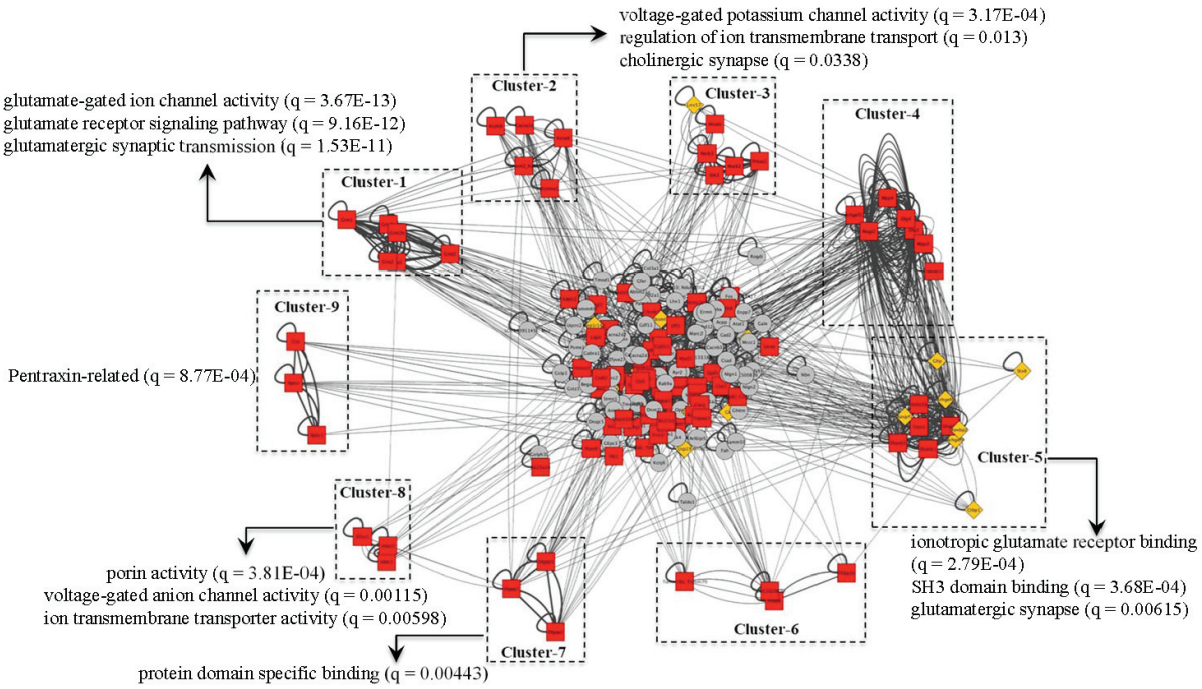

Table 1. Results of PantherDB analysis for the comparison between sham and acquisition groups

	PANTHER GO-Slim Pathways	over/ under	Fold Enrichment	Raw P-value	FDR (q-value)
Cellular Component	postsynaptic membrane (GO:0045211)	+	30.25	9.68E-11	3.10E-09
	neuromuscular junction (GO:0031594)	+	25.21	3.67E-04	2.14E-03
	synapse (GO:0045202)	+	12.67	2.09E-11	1.34E-09
	dendrite (GO:0030425)	+	9.71	7.15E-07	9.15E-06
	neuron projection (GO:0043005)	+	7.03	8.27E-09	1.77E-07
	cell junction (GO:0030054)	+	6.92	3.10E-04	1.98E-03
	cell projection (GO:0042995)	+	4.9	3.05E-07	4.88E-06
	integral to membrane (GO:0016021)	+	2.69	3.03E-05	2.42E-04
	plasma membrane (GO:0005886)	+	2.43	4.05E-06	3.70E-05
	cytoskeleton (GO:0005856)	+	2.31	9.41E-03	4.63E-02
	membrane (GO:0016020)	+	2.14	3.70E-06	3.94E-05
	protein complex (GO:0043234)	+	2.1	0.0001	7.14E-04
Biological Process	growth (GO:0040007)	+	44.12	9.25E-05	2.51E-03
	asymmetric protein localization (GO:0008105)	+	35.29	1.58E-04	3.86E-03
	muscle organ development (GO:0007517)	+	26.14	3.03E-07	1.85E-05
	neuron-neuron synaptic transmission (GO:0007270)	+	13.07	1.27E-08	1.55E-06
	pyrimidine nucleobase metabolic process (GO:0006206)	+	11.39	2.91E-03	3.55E-02
	synaptic transmission (GO:0007268)	+	6.38	4.01E-11	9.80E-09
	ion transport (GO:0006811)	+	4.48	2.13E-06	8.66E-05
	cell-cell signaling (GO:0007267)	+	4.43	2.12E-08	1.72E-06
	cytoskeleton organization (GO:0007010)	+	3.22	1.35E-03	2.20E-02
	protein localization (GO:0008104)	+	2.88	1.20E-03	2.08E-02
	transport (GO:0006810)	+	2.35	4.58E-06	1.60E-04
	localization (GO:0051179)	+	2.34	9.21E-07	4.50E-05
	neurological system process (GO:0050877)	+	2.11	3.25E-04	7.21E-03
	system process (GO:0003008)	+	2.05	4.42E-04	8.30E-03
	phosphate-containing compound metabolic process (GO:0006796)	+	1.94	1.45E-03	2.09E-02
	cellular component organization (GO:0016043)	+	1.76	2.71E-03	3.48E-02
	cell communication (GO:0007154)	+	1.55	3.25E-03	3.77E-02
	sensory perception of smell (GO:0007608)	-	< 0.01	2.15E-03	2.92E-02
	sensory perception of chemical stimulus (GO:0007606)	-	< 0.01	1.44E-03	2.19E-02
	sensory perception (GO:0007600)	-	< 0.01	0.000426	0.00866
Molecular Function	glutamate receptor activity (GO:0008066)	+	22.96	7.33E-09	3.50E-07
	nucleotide kinase activity (GO:0019201)	+	20.17	1.16E-06	3.70E-05
	voltage-gated calcium channel activity (GO:0005245)	+	13.07	2.02E-03	3.51E-02
	ligand-gated ion channel activity (GO:0015276)	+	9.8	3.71E-08	1.42E-06
	voltage-gated ion channel activity (GO:0005244)	+	8.11	1.37E-04	2.91E-03
	voltage-gated potassium channel activity (GO:0005249)	+	7.59	2.34E-03	3.44E-02
	ion channel activity (GO:0005216)	+	7.13	1.86E-11	3.56E-09
	cation channel activity (GO:0005261)	+	5.12	3.51E-03	4.19E-02
	small GTPase regulator activity (GO:0005083)	+	4.64	2.25E-03	3.59E-02
	transmembrane transporter activity (GO:0022857)	+	3.8	4.03E-09	3.84E-07
	transporter activity (GO:0005215)	+	3.54	4.84E-09	3.08E-07
	GTPase activity (GO:0003924)	+	3.13	1.67E-03	3.19E-02
	kinase activity (GO:0016301)	+	2.52	2.41E-03	3.29E-02
	pyrophosphatase activity (GO:0016462)	+	2.38	3.84E-03	4.31E-02
	catalytic activity (GO:0003824)	+	1.74	3.98E-06	1.08E-04
	protein binding (GO:0005515)	+	1.64	0.00313	0.0399

*: See Extended Table 1-1 for all Reactome pathway terms identified from the comparison between sham and acquisition groups

Table 2. Results of PantherDB analysis for the comparison between sham and retrieval groups

	PANTHER GO-Slim Pathways	over/ under	Fold Enrichment	Raw P-value	FDR (q-value)
Cellular Component	postsynaptic membrane (GO:0045211)	+	14.71	9.98E-09	7.99E-08
	neuromuscular junction (GO:0031594)	+	11.03	3.83E-03	1.29E-02
	proton-transporting ATP synthase complex (GO:0045259)	+	9.8	1.20E-03	4.51E-03
	synapse (GO:0045202)	+	8.31	1.24E-12	7.96E-11
	mitochondrial inner membrane (GO:0005743)	+	7.1	4.77E-09	5.08E-08
	dendrite (GO:0030425)	+	7.08	1.49E-08	1.06E-07
	SNARE complex (GO:0031201)	+	6.06	5.75E-03	1.84E-02
	neuron projection (GO:0043005)	+	5.33	2.61E-11	5.57E-10
	cell junction (GO:0030054)	+	5.05	5.70E-05	2.60E-04
	axon (GO:0030424)	+	4.68	1.31E-02	3.98E-02
	cell projection (GO:0042995)	+	3.75	7.41E-09	6.77E-08
	protein complex (GO:0043234)	+	2.31	8.91E-12	2.85E-10
	cytoskeleton (GO:0005856)	+	2.2	5.35E-04	2.14E-03
	membrane (GO:0016020)	+	1.99	1.14E-09	1.46E-08
	integral to membrane (GO:0016021)	+	1.87	5.15E-04	2.20E-03
	macromolecular complex (GO:0032991)	+	1.79	2.02E-07	1.17E-06
	cytoplasm (GO:0005737)	+	1.76	5.38E-10	8.61E-09
	plasma membrane (GO:0005886)	+	1.59	1.62E-03	5.77E-03
	cell part (GO:0044464)	+	1.44	1.96E-07	1.25E-06
	intracellular (GO:0005622)	+	1.37	2.18E-05	1.07E-04
Biological Process*	growth (GO:0040007)	+	19.3	1.01E-03	8.82E-03
	asymmetric protein localization (GO:0008105)	+	15.44	1.70E-03	1.34E-02
	oxidative phosphorylation (GO:0006119)	+	10.89	2.67E-08	9.31E-07
	pyrimidine nucleobase metabolic process (GO:0006206)	+	8.3	5.69E-04	6.31E-03
	JNK cascade (GO:0007254)	+	8.04	6.47E-04	6.32E-03
	respiratory electron transport chain (GO:0022904)	+	7.35	3.03E-09	1.48E-07
	generation of precursor metabolites and energy (GO:0006091)	+	6.03	1.52E-11	3.72E-09
	neuron-neuron synaptic transmission (GO:0007270)	+	5.72	2.13E-05	3.25E-04
	purine nucleobase metabolic process (GO:0006144)	+	5.63	4.04E-04	4.93E-03
	glycolysis (GO:0006096)	+	5.51	1.15E-03	9.39E-03
	mitochondrial transport (GO:0006839)	+	5.48	3.06E-03	1.86E-02
	neurotransmitter secretion (GO:0007269)	+	4.98	1.46E-04	1.98E-03
	cation transport (GO:0006812)	+	4.24	1.89E-03	1.44E-02
	calcium-mediated signaling (GO:0019722)	+	4.14	2.14E-03	1.45E-02
	mitochondrion organization (GO:0007005)	+	4	2.56E-03	1.65E-02
	synaptic transmission (GO:0007268)	+	3.99	5.54E-10	4.51E-08
	anatomical structure morphogenesis (GO:0009653)	+	3.68	6.22E-04	6.60E-03
	protein targeting (GO:0006605)	+	3.47	5.29E-04	6.15E-03
	ion transport (GO:0006811)	+	2.87	1.82E-05	2.96E-04
	cell-cell signaling (GO:0007267)	+	2.86	3.92E-07	9.58E-06
Molecular Function*	glutamate receptor activity (GO:0008066)	+	11.3	3.82E-07	9.12E-06
	nucleotide kinase activity (GO:0019201)	+	10.29	1.32E-05	1.94E-04
	SNAP receptor activity (GO:0005484)	+	7.35	3.07E-03	2.66E-02
	hydrogen ion transmembrane transporter activity (GO:0015078)	+	7.05	4.00E-06	8.48E-05
	carbohydrate kinase activity (GO:0019200)	+	6.64	4.27E-03	3.26E-02
	anion channel activity (GO:0005253)	+	5.25	3.61E-03	2.87E-02
	ligand-gated ion channel activity (GO:0015276)	+	5.07	4.31E-06	8.24E-05
	voltage-gated ion channel activity (GO:0005244)	+	4.14	2.14E-03	2.27E-02
	ion channel activity (GO:0005216)	+	4.06	5.90E-09	3.76E-07
	cation channel activity (GO:0005261)	+	3.58	2.49E-03	2.51E-02
	microtubule binding (GO:0008017)	+	3.4	5.95E-03	4.37E-02
	small GTPase regulator activity (GO:0005083)	+	3.39	1.12E-03	1.34E-02
	oxidoreductase activity (GO:0016491)	+	3	5.89E-08	1.88E-06
	kinase activity (GO:0016301)	+	2.79	2.71E-07	7.39E-06
	calcium ion binding (GO:0005509)	+	2.79	2.80E-03	2.54E-02

*: See Extended Table 2-1 for all GO-slim pathway terms

Table 3. Results of DAVID Bioinformatics analysis for the comparison between sham and acquisition groups

Cluster	Functional Annotation Term Summary*	Enrichment Score	FDR (q value)			
			Median	SD	Lowest	Highest
1	Postsynaptic membrane	13.96	5.88E-13	0.055	1.65E-20	0.18
2	Synapse	12.40	6.63E-12	0.041	1.65E-20	0.092
3	Ion transport	9.54	3.25E-07	4.75E-07	1.49E-07	1.05E-06
4	Mitochondrial inner membrane	7.44	0.0154	0.093	2.25E-12	0.19
5	Positive regulation of excitatory postsynaptic potential	5.23	0.0014	0.848	3.79E-04	1.47
6	Neuronal membrane-associated guanylate kinases	5.16	0.0163	0.224	4.25E-04	0.46
7	PDZ and SH3 domains	4.91	0.0121	19.78	1.44E-07	65.75
8	Ionotropic glutamate and NMDA receptors	4.86	0.0272	0.859	3.01E-04	1.50
9	AMPA glutamate receptor complex	4.42	0.0104	5.28	0.0018	9.15
10	Glutamatergic synapses	4.34	0.1636	25.26	1.44E-07	100.0
11	Guanylate-kinase-associated protein	4.25	1.0843	0.682	4.25E-04	1.26

*: See Extended Table 3-1 for detailed functional clustering annotation terms